EPJ Web of Conferences **276**, 01028 (2023) https://doi.org/10.1051/epjconf/202327601028
SQM 2022

Insights into the initial conditions and evolution of hadronic collisions with flow observables.

Vytautas Vislavicius[1,*]

[1]Lund University, Sweden

Abstract. Studies of anisotropic flow in heavy-ion collisions are one of the critical elements in understanding the production and evolution of the Quark Gluon Plasma. These proceedings review the most recent results on anisotropic flow measurements at the LHC energies. In particular, recent measurements of p_{T}-differential $v_2\{4\}$ in Pb–Pb collisions for a plethora of light-flavour particles are discussed and compared to models with and without partonic coalescence. The measurements of $v_2\{2\}$ and $v_2\{4\}$ allow for the calculation of relative flow fluctuations, which for the first time are also reported for (multi)strange baryons. The study is further extended to higher moments of the underlying charged-particle v_2 PDF, where a transition from non-Gaussian to Gaussian fluctuations is observed. Finally, the correlation between v_2 and mean transverse momentum $[p_{\mathrm{T}}]$ is studied in terms of the Pearson Correlation Coefficient. This opens new venues to study nuclear deformation in ultra-central heavy-ion collisions and could provide a tool to identify processes in the pre-QGP phase.

1 Introduction

Studies of anisotropies in azimuthal distributions of particles produced in heavy-ion collisions have significantly contributed to the understanding of the hot and dense quark-gluon plasma (QGP). In particular, the anisotropies of energy density in the initial state give rise to large pressure gradients, which drive the expansion of the QGP. On a macroscopic level, the evolution of the QGP is described by relativistic hydrodynamics, typically studied in terms of anisotropic flow coefficients v_n, which measure the momentum anisotropy of final state particles. Experimentally the hydrodynamical prescription has been observed to be dominant at low transverse momenta ($p_{\mathrm{T}} \lesssim 3\,\mathrm{GeV}/c$).

One of the outcomes of the hydrodynamical evolution of the system is the (inverse) mass-ordering of flow coefficients v_n at low p_{T}. This has been experimentally observed as, for example, $v_2^{\pi} \gg v_2^{p}$ [1] and is due to heavier particles receiving a larger boost from the flowing medium. On the other hand, at large momenta ($p_{\mathrm{T}} \gtrsim 10\,\mathrm{GeV}/c$) where no mass-ordering has been observed [2] the dominant source for non-zero v_n is jet quenching. The transition from hydrodynamics and jet-dominated v_n occurs in the intermediate p_{T} region, $3 \lesssim p_{\mathrm{T}}/(\mathrm{GeV}/c) \lesssim 10$, where other processes such as partonic coalescence might contribute.

A common way to measure anisotropic flow coefficients in hadronic collisions is using Q-cumulants calculated from multi-particle correlations [3]. The advantage of this method is that different orders of correlations exhibit different sensitivity to the moments of underlying

*e-mail: vytautas.vislavicius@cern.ch

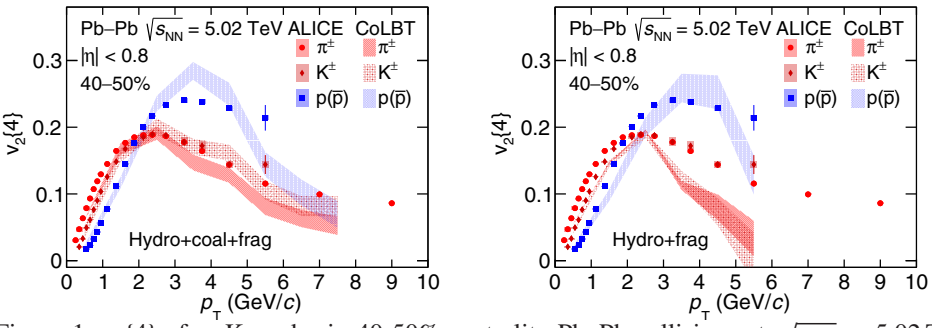

Figure 1: $v_2\{4\}$ of π, K, and p in 40-50% centrality Pb–Pb collisions at $\sqrt{s_{\rm NN}} = 5.02\,\text{TeV}$. Shaded bands show predictions from CoLBT model [8] with (left) and without (right) coalescence. Figure from [7].

v_n probability density function (PDF). As a result, from the measurement of v_n with 2- and 4-particle correlations ($v_n\{2\}$ and $v_n\{4\}$, respectively) one can calculate relative flow fluctuations as prescribed in [3]. On the other hand, measurements of particle correlations also receive contributions from non-flow effects such as jet fragmentation, jet quenching, and decays of resonance hadrons. To suppress the short-range correlations, one usually introduces a minimum separation in pseudorapidity, $|\Delta\eta|$, between the correlated particles. Alternatively, measurements of higher-order cumulants have also been shown to be less sensitive to non-flow effects [4].

2 Anisotropic flow in Pb–Pb collisions at $\sqrt{s_{\rm NN}} = 5.02\,\text{TeV}$

Recently, the ALICE Collaboration [5, 6] has reported on $p_{\rm T}$-differential measurements of v_2 for identified particles, shown in Fig. 1 [7]. This is the first measurement of $v_2\{4\}$ that includes (multi) strange hyperons, although, in these proceedings, only π, K, and p are considered for brevity. At lower transverse momenta, $p_{\rm T} \lesssim 2\,\text{GeV}/c$ $v_2\{4\}$ exhibits an inverse mass ordering, $v_2^{\pi}\{4\} > v_2^{K}\{4\} > v_2^{p}\{4\}$. The same holds for hyperons as reported in [7]. This is expected from hydrodynamics, where heavier particles receive a larger boost in $p_{\rm T}$ from the common velocity field. Around $p_{\rm T} \approx 2\,\text{GeV}/c$, we see a characteristic crossing, above which $v_2\{4\}$ is grouped between baryons and mesons. The grouping is understood in terms of coalescence, where a combination of three partons results in a larger momentum of a hadron than a combination of two partons.

The measured $v_2\{4\}$ for different particle species is also compared to predictions of CoLBT model [8]. In particular, two cases are considered: one where the evolution of QGP follows hydrodynamics and fragmentation, and the other where quarks are allowed to coalesce before hadronization. At low $p_{\rm T}$ we see that hydrodynamics alone underestimates the $v_2\{4\}$ for all particle species. The description of the data is significantly better once coalescence is considered. Note that even with coalescence, the model underestimates the $v_2\{4\}$ of π; this could be due to a large number of π coming from the decays of short-lived heavy resonances, where a fraction of flow builds up before the decay.

The crossing between baryons and mesons at $p_{\rm T} \approx 2\,\text{GeV}/c$ is present in both models. While it comes out naturally from coalescence, in the hydro+frag model, this crossing is facilitated by a mass-dependent $p_{\rm T}$ value where fragmentation starts to dominate over hydrodynamics. It therefore suggests that the observed baryon/meson crossing is not unique to quark coalescence. Nevertheless, at larger transverse momenta ($p_{\rm T} \gtrsim 3\,\text{GeV}/c$) we find that fragmentation alone predicts a sharp decrease in $v_2\{4\}$, a trend which is not observed in the data.

On the other hand, the model including quark coalescence provides a significantly better description, although the absolute values for π and p are still underestimated. Finally, it is also worth noting that the CoLBT model does not consider jet quenching, which could further modify $v_2\{4\}$ at larger p_{T} values.

2.1 Flow fluctuations

Measurements of $v_2\{2\}$ and $v_2\{4\}$ allow for the estimation of relative flow fluctuations $F(v_2) = \sigma(v_2)/\langle v_2 \rangle$. For the first time these have been reported for identified particles in [7] and are shown for several centrality classes in Fig. 2. No apparent species dependence is observed in central collisions, where $F(v_2)$ shows little evolution with p_{T}. In more peripheral collisions starting from 30-40% centrality, a species dependence emerges and, in particular, $F(v_2)$ of baryons and mesons show a non-monotonic evolution with minima at different p_{T}. The baryon/meson grouping seen in v_2 is also present in $F(v_2)$, but occurs at lower transverse momenta. The emerging species and p_{T}-dependence of $F(v_2)$ suggest that $\sigma(v_2)$ is also sensitive to final state interactions.

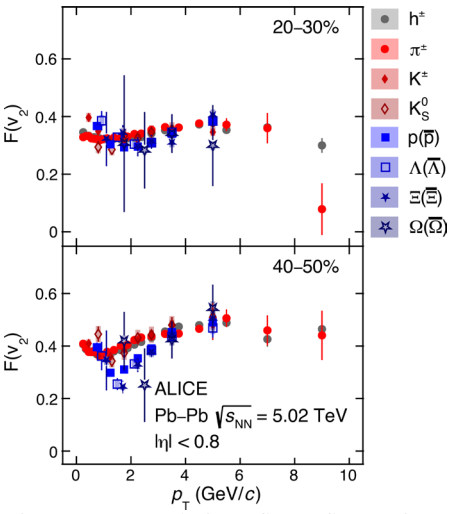

Figure 2: Relative flow fluctuations of identified hadrons in two centrality classes in Pb–Pb collisions at $\sqrt{s_{\mathrm{NN}}}$ = 5.02 TeV. Figure from [7].

Measuring the underlying PDF of v_2 allows us to probe the initial geometry of the collision. The higher moments of the v_2 PDF can be calculated from the measurements of v_2 using higher orders of particle correlations as prescribed in [10]. The CMS Collaboration has reported on p_{T}-integrated skewness (γ_1) and kurtosis (γ_2) of charged hadrons as a function of centrality in Pb–Pb collisions at $\sqrt{s_{\mathrm{NN}}}$ = 5.02 TeV [9]. In addition, the contributions coming from the higher moments have been removed from the reported γ_1 and γ_2, see Fig. 3. This contribution appears to be larger for γ_1 and generally results in steeper slopes of γ_n with centrality.

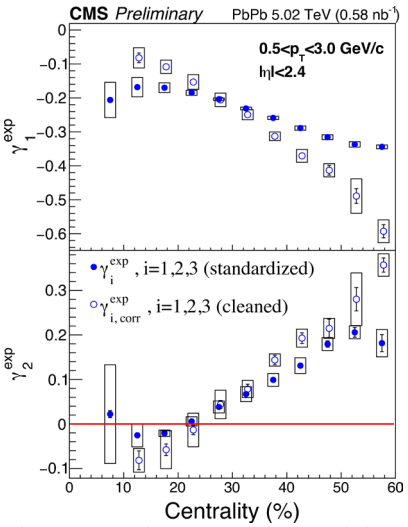

Figure 3: Skewness (top) and kurtosis (bottom) of the underlying v_2 PDF in Pb–Pb collisions at $\sqrt{s_{\mathrm{NN}}}$ = 5.02 TeV. Figure from [9].

The skewness of the v_2 PDF is negative in the whole centrality range and reduces in more peripheral collisions. The negative values of γ_1 originate from a larger tail of the v_2 distribution at lower values [11], and the data suggests that this effect is enhanced with increasing centrality. The kurtosis γ_2 is small up to 20% centrality and rises as collisions get more peripheral. Overall, the non-zero γ_1 and γ_2 suggest non-Gaussian fluctuations of v_2.

To first order, v_2 is a linear response to the eccentricity ϵ_2 of the initial state. In practice, the hydrodynamical expansion of the QGP could also modify the underlying PDF. This is

studied by the ALICE Collaboration, where γ_1 and γ_2 are measured as a function of p_{T}, see Fig. 4. Interestingly, the negative (positive) values of γ_1 (γ_2) are only seen at $p_{\mathrm{T}} \lesssim 3\,\mathrm{GeVc}$. The observed p_{T}-dependence suggests that the v_2 PDF is modified in a non-trivial way and thus the exact linear response $v_n = \kappa\epsilon_n$ breaks down. At higher transverse momenta, γ_1 and γ_2 are consistent with zero and thus v_2 fluctuations become Gaussian. Finally, it is worth noting that the observed p_{T}-dependence of skewness and kurtosis is observed in the same region where $F(v_2)$ exhibits baryon/meson grouping, and it would therefore be interesting to measure these moments for identified particles.

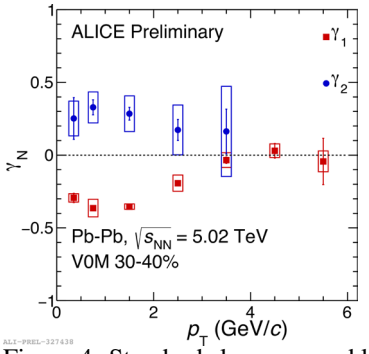

Figure 4: Standard skewness and kurtosis as a function of p_{T} in Pb–Pb collisions at $\sqrt{s_{\mathrm{NN}}}$ = 5.02 TeV and 30-40% centrality.

3 Correlations between v_2 and $[p_{\mathrm{T}}]$

Recently, the correlation between the mean transverse momentum $[p_{\mathrm{T}}]$ and v_2 gained popularity as a tool to study the initial state of heavy-ion collisions. It is studied in terms of the Pearson Correlation Coefficient, $\rho_2 \equiv \rho\left(v_2^2, [p_{\mathrm{T}}]\right)$, where $[p_{\mathrm{T}}]$ is calculated on an event-by-event basis and in a limited kinematic region. The $[p_{\mathrm{T}}]$ in the hydrodynamic regime is driven by the radial flow and thus is expected to increase as collisions become more central. At the same time, the elliptic component driving v_2 becomes less pronounced and in the most central collisions originates predominantly from local density fluctuations and the deformation of projectile nuclei. This can be used to study the nuclear deformation of heavy ions, as discussed in [12].

The measured ρ_2 in Pb–Pb and Xe–Xe collisions at $\sqrt{s_{\mathrm{NN}}}$ = 5.02 and 5.44 TeV, respectively, is reported by ALICE in [13] and shown in Fig. 5 together with comparisons to different models. The sharp drop in ρ_2 in the most central collisions is smeared out by choice of a wider centrality class, 0-5%, but the decreasing trend at low centralities is seen nevertheless. In semi-central collisions (10-60%) the correlation shows little evolution with centrality and is higher in Pb–Pb collisions compared to Xe–Xe. Comparing the ρ_2 in Pb–Pb to different models, we find that in the 0-15% centrality range the data is described by all the models considered. However, Trajectum [14], Jetscape [15], and v-USPhydro [16] predict a decreasing trend beyond 15% centrality, which clearly is not in agreement with the Pb–Pb data. On the other hand, the IP-Glasma [17] initial conditions, where gluon distributions are estimated from Color Glass Condensate (CGC) calculations, coupled to hydrodynamics code MUSIC [18, 19] and UrQMD [20, 21] provides a qualitatively correct description of the measurement in Pb–Pb collisions. A similar conclusion can be drawn for measurements in Xe–Xe, but here the Xe nucleus in the IP-Glasma prescription is modelled as a spherical ($\beta_2 = 0$) or as a deformed ($\beta_2 = 0.16$) nucleus. The deformation parameter $\beta_2 = 0.16$ for the Xe nucleus has been previously predicted in [22] and tested in [23] using measurements of anisotropic flow. While β_2 does not have any significant effect on ρ_2 in semi-central collisions, in the 0-5% centrality class where deformation effects are most pronounced, the IP-Glasma model with $\beta_2 = 0.16$ is preferred.

On the other hand, ρ_2 can also be used to probe the fundamental processes leading to the formation of the QGP. From purely geometrical considerations, with decreasing multiplicity, the transverse size of the initial state reduces while the eccentricity grows. This drives ρ_2 towards lower values, ultimately changing the sign of the correlation. As proposed

in [24], at sufficiently low multiplicity ρ_2 could probe initial momentum correlations. These can originate from novel processes leading to the pre-QGP phase, such as the Color Glass Condensate. In particular, for a fixed multiplicity, events with larger $[p_T]$ typically have smaller transverse sizes. In the CGC picture, this reduces the number of color domains, which in turn enhances the initial momentum anisotropy [25] and results in positive values of ρ_2. The initial momentum correlations are weak and could only dominate over geometry at very low multiplicities. This would result in ρ_2 being positive at the lowest multiplicity, decreasing steeply as collisions become more central (competition between initial momentum- and geometry-dominated ρ_2), then changing the slope from negative to positive and following geometry-only driven ρ_2.

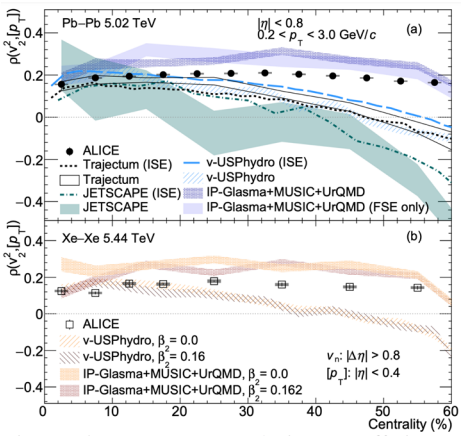

Figure 5: Pearson Correlation Coefficient of v_2 and $[p_T]$ as a function of centrality in Pb–Pb (top) and Xe–Xe collisions at $\sqrt{s_{NN}}$ = 5.02 and 5.44 TeV, respectively. Figure from [13].

By now, multiple collaborations have reported on measurements of ρ_2. The measurement by ALICE is shown in Fig. 6, where both Pb–Pb and pp collisions at $\sqrt{s_{NN}}$ = 5.02 and 13 TeV, respectively, are compared to different MC models. The measured ρ_2 is positive in the whole multiplicity region considered and is very similar in Pb–Pb and pp collisions. The change of slope in Pb–Pb collisions is observed at significantly larger multiplicity, $N_{ch}(|\eta| < 0.8) \approx 100$, as compared to the CGC-inspired model where the slope changes at around $N_{ch}(|\eta| < 0.8) \approx 20$. Moreover, IP-Glasma + MUSIC + UrQMD predicts a rapid change of ρ_2 at low multiplicity while the evolution seen in data is less pronounced. The similarities between pp and Pb–Pb data at comparable N_{ch} suggest that the mechanism giving rise to $[p_T]$-v_2 correlations in the two systems might be the same. It is also interesting to see that AMPT predicts the decreasing trend of ρ_2 at $N_{ch}(|\eta| < 0.8) \lesssim 130$, suggesting that the change of slope is not unique to CGC initial conditions. In both data and the models considered, the rise of ρ_2 at the lowest multiplicities could result from non-flow, but this requires further studies.

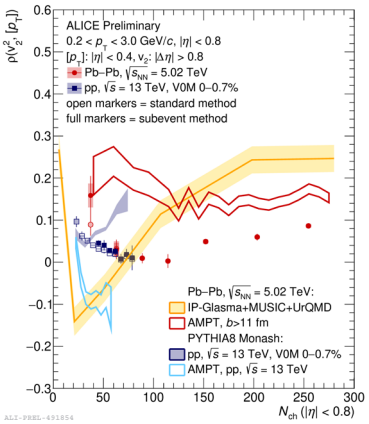

Figure 6: Pearson Correlation Coefficient of v_2 and $[p_T]$ as a function of $N_{ch}(|\eta| < 1.6)$ in Pb–Pb and high multiplicity pp collisions at $\sqrt{s_{NN}}$ = 5.02 and 13 TeV, respectively, in comparison to multiple model predictions.

Finally, the ATLAS Collaboration reported on sensitivity to the kinematic region where ρ_2 is measured[1] [26]. As shown in Fig. 7, lower p_T results in systematically smaller values of ρ_2, which is most pronounced in semi-central collisions. Reducing the η acceptance from 5 to 2 units of pseudorapidity modifies ρ_2 in a non-trivial way. Most notably, the change from

[1]Note that the ATLAS measurements are reported as a function of centrality and are performed in a different kinematic range as compared to ALICE, and so direct comparison of the results is currently not possible.

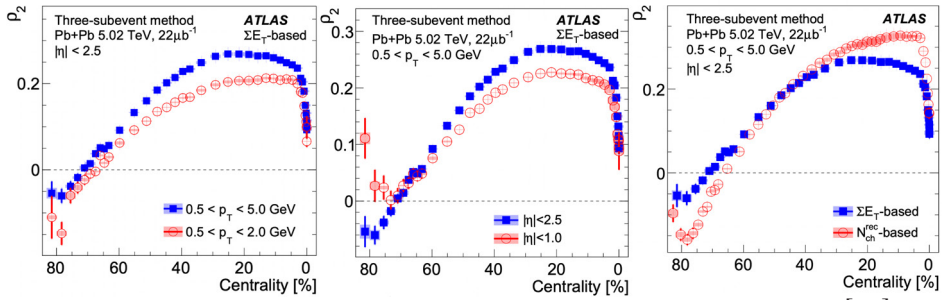

Figure 7: Centrality dependence of the Pearson Correlation Coefficient of v_2 and $[p_T]$ in Pb–Pb collisions at $\sqrt{s_{NN}} = 5.02$ TeV, measured in different p_T regions (left), different η regions (middle), and using different centrality estimators (right). Figure from [26].

decreasing to increasing trend is observed at lower centrality values for a smaller acceptance. This is possibly due to larger non-flow contamination due to a smaller $|\Delta\eta|$ separation. At the same time, it is not obvious whether initial momentum correlations can survive longitudinal decorrelation, and thus a large $|\Delta\eta|$ gap could also destroy them. Finally, the ρ_2 measured using two different centrality estimators by ATLAS are also compared in Fig. 7, where the ΣE_T-based estimator classifies events into centrality classes based on the total energy deposited into forward calorimeters and the N_{ch}-based classification depends on the total number of charged particles reconstructed at midrapidity. It is found that the N_{ch}-based estimator results in a steeper slope of ρ_2 and a more rapid change of behaviour within 75%-80% centrality. This is likely due to the finite resolution of the event activity, where midrapidity-based estimators are more sensitive to event-by-event fluctuations. Similar observations were previously reported in a model-inspired study [27], albeit at significantly lower center-of-mass energies and collision systems. These findings indicate that a more thorough model study is required to understand whether the observed signal in the data is unique to new phenomena or is an artefact of more basic kinematic considerations.

4 Summary

Measurements of the anisotropic flow at the LHC have significantly expanded our understanding of the production and evolution of the QGP. First measurements of $v_2\{4\}$ for a plethora of identified particles show a mass ordering at low p_T and baryon/meson grouping at higher momenta. The trends observed in the data are qualitatively described by hydrodynamic models that consider partonic coalescence. The baryon/meson grouping is also observed in the relative flow fluctuations, but it occurs at significantly lower p_T, suggesting it is of a different origin. The higher moments of the inclusive particle v_2 distribution indicate non-Gaussian fluctuations in the same p_T region where baryon/meson grouping is observed for $F(v_2)$, and they become Gaussian at $p_T \gtrsim 3\,\text{GeV}/c$. This calls for future measurements of γ_1 and γ_2 for identified particles. Finally, measurements of $v_2 - [p_T]$ correlations open new venues to study nuclear deformation and processes leading to the formation of the QGP. Measurements of ρ_2 in central Pb–Pb and Xe–Xe collisions suggest the deformation parameter of Xe nucleus $\beta_2 = 0.16$, which different methods have previously confirmed. The evolution of ρ_2 with centrality shows trends that are qualitatively better described by models that utilize IP-Glasma in the initial state. In ultraperipheral heavy-ion collisions, indications of a ρ_2 slope change are observed. However, this effect cannot be uniquely attributed to initial momentum correlations, and a better understanding of biases originating from the kinematic selections is required.

References

[1] B.B. Abelev et al. (ALICE), JHEP **06**, 190 (2015), 1405.4632
[2] B. Abelev et al. (ALICE), Phys. Lett. B **719**, 18 (2013), 1205.5761
[3] A. Bilandzic, C.H. Christensen, K. Gulbrandsen, A. Hansen, Y. Zhou, Phys. Rev. C **89**, 064904 (2014), 1312.3572
[4] S. Acharya et al. (ALICE), JHEP **07**, 103 (2018), 1804.02944
[5] K. Aamodt et al. (ALICE), JINST **3**, S08002 (2008)
[6] B.B. Abelev et al. (ALICE), Int. J. Mod. Phys. A **29**, 1430044 (2014), 1402.4476
[7] S. Acharya et al. (ALICE) (2022), 2206.04587
[8] W. Chen, S. Cao, T. Luo, L.G. Pang, X.N. Wang, Phys. Lett. B **810**, 135783 (2020), 2005.09678
[9] Tech. rep., CERN, Geneva (2022), https://cds.cern.ch/record/2806158
[10] R.S. Bhalerao, G. Giacalone, J.Y. Ollitrault, Phys. Rev. C **99**, 014907 (2019), 1811.00837
[11] G. Giacalone, L. Yan, J. Noronha-Hostler, J.Y. Ollitrault, Phys. Rev. C **95**, 014913 (2017), 1608.01823
[12] G. Giacalone, Phys. Rev. C **102**, 024901 (2020), 2004.14463
[13] S. Acharya et al. (ALICE), Phys. Lett. B **834**, 137393 (2022), 2111.06106
[14] G. Nijs, W. van der Schee, U. Gürsoy, R. Snellings, Phys. Rev. Lett. **126**, 202301 (2021), 2010.15130
[15] D. Everett et al. (JETSCAPE), Phys. Rev. Lett. **126**, 242301 (2021), 2010.03928
[16] J. Noronha-Hostler, J. Noronha, M. Gyulassy, Phys. Rev. C **93**, 024909 (2016), 1508.02455
[17] B. Schenke, P. Tribedy, R. Venugopalan, Phys. Rev. C **86**, 034908 (2012), 1206.6805
[18] B. Schenke, S. Jeon, C. Gale, Phys. Rev. C **82**, 014903 (2010), 1004.1408
[19] J.F. Paquet, C. Shen, G.S. Denicol, M. Luzum, B. Schenke, S. Jeon, C. Gale, Phys. Rev. C **93**, 044906 (2016), 1509.06738
[20] S.A. Bass et al., Prog. Part. Nucl. Phys. **41**, 255 (1998), nucl-th/9803035
[21] M. Bleicher et al., J. Phys. G **25**, 1859 (1999), hep-ph/9909407
[22] P. Möller, A.J. Sierk, T. Ichikawa, H. Sagawa, Atom. Data Nucl. Data Tabl. **109-110**, 1 (2016), 1508.06294
[23] S. Acharya et al. (ALICE), Phys. Lett. B **784**, 82 (2018), 1805.01832
[24] G. Giacalone, B. Schenke, C. Shen, Phys. Rev. Lett. **125**, 192301 (2020), 2006.15721
[25] T. Lappi, B. Schenke, S. Schlichting, R. Venugopalan, JHEP **01**, 061 (2016), 1509.03499
[26] G. Aad et al. (ATLAS) (2022), 2205.00039
[27] J. Jia, S. Huang, C. Zhang, Phys. Rev. C **105**, 014906 (2022), 2105.05713